A Comparative Study of Mesophase Formation in Rigid Chain Polyesters with Flexible Side Chains

J. M. Rodriguez-Parada, R. Duran, and G. Wegner*

Max-Planck-Institut für Polymerforschung, Postfach 3148, D-6500 Mainz, F.R.G.
Received September 6, 1988; Revised Manuscript Received November 4, 1988

ABSTRACT: Two series of rigid chain polyesters having flexible linear side chains from 6 to 16 carbon atoms were synthesized and studied by optical microscopy, differential scanning calorimetry, and X-ray diffraction. They were prepared by melt condensation polymerization of 2,5-dialkoxyhydroquinones with terephthalic acid in one case and with bicyclo[2.2.2]octane-1,4-dicarboxylic acid in the other. Thus one series of polymers has a wholly aromatic backbone while the other contains alternating rigid aliphatic and aromatic units. Both series show a low-temperature solid–solid transition attributed to the disordering of the side chains and similar melting temperatures, which decrease accordingly as the length of the side chains increases. However, while the polymers from bicyclo[2.2.2]octane-1,4-dicarboxylic acid melt into an isotropic liquid, most of the terephthalic acid polyesters melt into a liquid crystalline phase, thus suggesting that interchain interactions provided by the wholly aromatic backbone are necessary for the stabilization of a mesophase in this class of materials. In the solid state both series of polymers crystallize into similar layered structures. X-ray diffraction shows that the layer spacing increases linearly with increasing length of the side chains, and comparison with molecular dimensions suggests that the side chains are interdigitated and tilted with respect to the backbone. Wholly aromatic polyesters containing four flexible side chains per repeat unit were also prepared. When the side chains are of equal length, the material is highly crystalline and melts directly into an isotropic liquid. X-ray analysis indicates a bilayer structure in the solid state in which the side chains are tilted with respect to the backbone but not interdigitated. When the side chains are of different length and alternating along the backbone, their crystallization is greatly suppressed, thus giving rise to a broad mesomorphic temperature range in which the side chains are disordered. Most of this disorder is preserved on cooling to the solid phase.

Introduction

In the past several years much interest has been devoted to the study of rigid chain macromolecules, mainly because of their superior mechanical properties. Many of these materials form mesomorphic phases on heating; however, their high melting points usually make them inaccessible for processing by conventional methods. To reduce the melting temperatures of these materials, several approaches, such as introduction into the main chain of bent, crankshaft-shaped, laterally substituted, and flexible units, have been used.[1,2] More recently, systematic studies on rigid polymers containing flexible side chains have been carried out.[3–8] They have shown not only that the melting temperatures decrease as the length of the side chains increases but also that these polymers are able to form novel layered mesophases.[9,10] The flexible alkyl side chains are thought to act as a bound solvent for the rigid polymeric backbone.[11]

Most of the rigid polymers containing flexible side chains synthesized up to now have been polyesters, polyamides, and polyimides, all containing aromatic residues. Aromatic units not only give the necessary rigidity to the backbone but also contain polarizable π electrons which can lead to strong intermolecular interactions, thus contributing to increasing the transition temperatures of these polymers. Only recently polyesters with flexible side chains in which some of the phenylene units in the aromatic chain were replaced by cyclohexylene units were reported.[12] This decreases considerably the transition temperatures; however, it also decreases the stiffness of the backbone. One approach to reduce interchain interactions while conserving the stiffness of the backbone would be the replacement of aromatic units by rigid aliphatic moieties such as bridgehead bicyclic compounds. A likely candidate would be bicyclo[2.2.2]octane, which is approximately the same length and width as a benzene ring, differing only in thickness.

The effect of replacing 1,4-phenylene units in low molecular weight liquid crystals by 1,4-bicyclo[2.2.2]octylene units has been studied by Dewar et al.[13–15] and by Gray et al.[16,17] In general, a widening of the nematic phase range was observed for most compounds, suggesting that the linear geometry of the bicyclo[2.2.2]octane, and the cylindrical symmetry it tends to induce on the rod-shaped molecules, was a factor stabilizing the mesophase.

Polyesters containing 1,4-bicyclo[2.2.2]octylene units have also been reported in the literature.[18–21] Most of these polymers melt at high temperatures with decomposition, although some were reported to show birefringent melts. However, the lack of a systematic and thorough characterization of these polymers does not allow any conclusions to be reached on the role of the 1,4-bicyclo[2.2.2]octylene unit in the mesomorphic properties of polymeric systems.

One of the goals of this work was to study the effect of substituting a 1,4-phenylene residue in the repeat unit of wholly aromatic polyesters containing flexible side chains by the 1,4-bicyclo[2.2.2]octylene moiety. In these systems, the flexible side chains should allow the transition temperatures to be lowered to a point where thermal decomposition is not a problem and a systematic characterization can be carried out. For this, two series of polyesters were synthesized: one from bicyclo[2.2.2]octane-1,4-dicarboxylic acid and 2,5-dialkoxyhydroquinones containing flexible side chains from 6 to 16 carbon atoms and the other from terephthalic acid with the same disubstituted hydroquinones. The chemical structures of the polymers are shown in Scheme I.

The series of polyesters based on terephthalic acid will also give the opportunity to compare them with a series of poly(1,4-phenylene-2,5-dialkoxyterephthalate)s that has been well-characterized and is reported in the literature.[4,5,10] These two series give a unique opportunity to probe the effect of substitution on the two different residues of the backbone repeat, since both series have identical backbones, the only difference being that in one series the side chains are attached to the hydroquinone residue while in the other they are attached to the terephthalic acid residue. Identical substitution on different

0024-9297/89/2222-2507$01.50/0

Table I
Yields, Melting Points, and Elemental Analysis of 2,5-Dialkoxybenzoquinones and Derivatives

	dialkoxybenzoquinones		dialkoxyhydroquinones		dialkoxyhydroquinone diacetates	
n^a	yield, %	mp, °C	yield, %	mp, °C	yield, %	mp, °C
6	39.0	135.0–136.0	88.0	99.5–100.0	92.0	74.5–75.0
8	57.3	131.5–132.0	98.0	97.0–97.5	90.5	75.5–76.0
10	69.3	126.5–127.5	94.5	100.0–101.0	87.3	84.0–85.0
12	55.5	123.5–124.5	87.5	102.0–103.0	91.0	91.5–92.5
14	90.0	121.0–122.0	89.4	104.5–105.5	93.5	95.5–96.0
16	80.5	119.5–120.5	80.0	107.0–108.0	83.5	96.0–97.0

[a] Number of carbon atoms in the side chain.

Scheme I

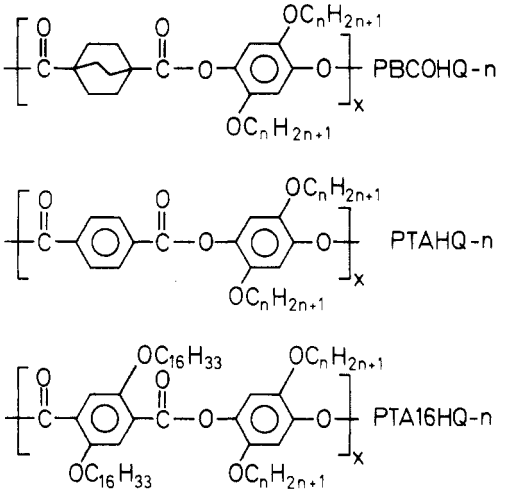

Scheme II

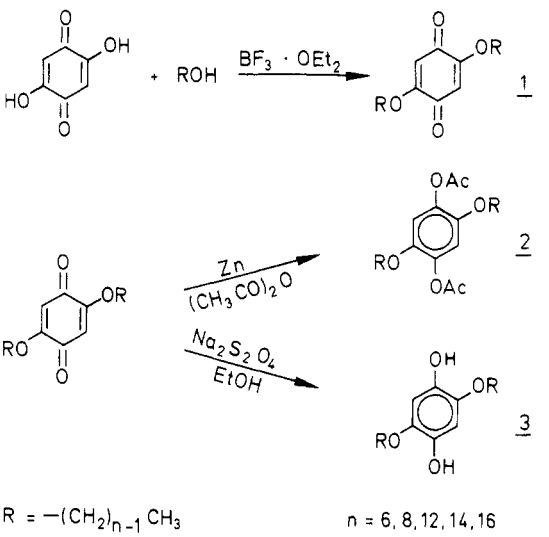

residues of the backbone repeat has been shown to cause considerable differences in the thermal properties of poly(*p*-phenyleneterephthalate)s.[2]

Another goal of this study was to investigate the effect of the number of flexible side chains per repeat unit on the liquid crystalline properties of this type of polymers. Previous work has examined the effect of one,[3,7,12] two,[4-6,10] and six[8,9] flexible side chains per repeat. We have made also two polyesters containing four flexible side chains per repeat unit. Their structure is also shown in Scheme I. Normally, increasing the number of side chains decreases the transition temperatures and increases the solubility; however, it has also led to a variety of mesomorphic structures. Another possibility that has not been exploited before is the incorporation of two alternating different length side chains into the same polymer backbone. This is expected to add disorder to the system, therefore lowering melting temperatures and perhaps increasing the liquid crystalline range. One of the polymers made with four side chains per repeat considers this case.

Results

The synthesis of the 2,5-substituted quinone derivatives required for the preparation of polyesters with flexible side chains is shown in Scheme II. In the first step 2,5-dialkoxy-*p*-benzoquinones were prepared from 2,5-dihydroxybenzoquinone and 1-alkanols in the presence of boron trifluoride etherate by a modification of a literature procedure.[22] The yields of this reaction were variable (40–90%), but rather good yields were obtained with the longer chain alcohols.

The reduction of the benzoquinones to the hydroquinones with sodium hyposulfite[23] was achieved in essentially 100% conversion, and high yields were obtained after purification. However, these materials oxidize slowly in air,[23] especially in solution during recrystallization, and should be kept in an inert atmosphere. The reductive acetylation of the corresponding benzoquinones[22] with zinc powder in acetic anhydride also worked in essentially 100% conversion to yield the stable hydroquinone diacetates, which were easily purified by recrystallization.

The yields and melting points of all the compounds prepared are collected in Table I.

Polyesters with flexible side chains containing the bicyclo[2.2.2]octane ring system were made by bulk condensation polymerization of bicyclo[2.2.2]octane-1,4-dicarboxylic acid with the corresponding 2,5-dialkoxyhydroquinone diacetates. Yields close to 90% were achieved in all cases. These polymers will be designated in the text following as PBCOHQ-*n*, where *n* is the number of carbon atoms in the side chain.

Attempts to polymerize terephthalic acid with 2,5-dialkoxyhydroquinone diacetates in the same manner as for the PBCOHQ-*n* polymers yielded only low molecular weight polyesters and dark decomposition products since both the reactivity of terephthalic acid and its solubility in the molten hydroquinone diacetates are lower than those of bicyclo[2.2.2]octane-1,4-dicarboxylic acid. Therefore, these polymers (PTAHQ-*n*) were prepared by the direct condensation of 2,5-dialkoxyhydroquinones with terephthaloyl chloride which melts at a lower temperature than that of the substituted hydroquinones. It is worth noting that the melt of terephthaloyl chloride with the 2,5-dialkoxyhydroquinones is initially deep red, probably owing to the formation of a charge-transfer complex, which disappears as the polymerization progresses, yielding at the end light-yellow polyesters.

In addition to these two series of polymers, which contain two flexible side chains per repeat unit, two polyesters containing four side chains per repeat were made. These

Table II
Characterization of Polymers from Bicyclo[2.2.2]octane-1,4-dicarboxylic Acid and 2,5-Dialkoxyhydroquinone Diacetates (PBCOHQ-*n*)

			thermal transitions[c]			
			heating		cooling	
n[a]	$[\eta]$[b]	layer spacing d, Å	T_s	T_m	T_s	T_m
6	1.10	10.1	63[d]	315		254
8	0.99	11.5	60[d]	255		210
10	1.21	12.8	55[d]	243		204
12	0.53	15.2	28	223	−2	186
14	0.87	16.5	46	206	30	166
16	0.59	17.8	60	193	49	160

[a] Number of carbon atoms in the side chain. [b] In dL/g, measured in CH_2Cl_2/TFA (95/5 (v/v)) at 20 °C. [c] In °C. Heating and cooling rates: 20 °C/min. [d] Transition observed only in the first heating scan.

were synthesized by condensation of 2,5-bis(hexadecyloxy)terephthalic acid chloride, prepared as described by Ballauff,[4] with 2,5-bis(hexadecyloxy)hydroquinone (PTA16HQ16) and 2,5-bis(hexyloxy)hydroquinone (PTA16HQ6), by the same procedure used for the polyesters of terephthalic acid described in the Experimental Section.

All the polymers were characterized by DSC, X-ray diffraction, and optical microscopy. The results are summarized in Tables II and III and are described in the following text.

PBCOHQ-*n* Polymers. PBCOHQ-*n* polymers having side chain lengths of 6, 8, 10, 12, 14, and 16 carbons were studied. Table II shows the intrinsic viscosities and transition temperatures observed. Figure 1 shows the heating and cooling DSC scans recorded for the 16-carbon side chain material. The DSC heating scan consists of two transitions with peaks at 60 and 193 °C. The cooling scan also consists of two peaks at 49 and 161 °C. Study of the higher temperature transition by polarizing optical microscopy showed that at this temperature the material melted from a birefringent solid to an isotropic melt. A bimodal shape of this melting peak was usually seen by DSC on materials crystallized from the melt. This seems to be typical for this type of polyesters[4,24] and has been attributed to different size crystallites and order present in these materials.

As shown in Table II, the PBCOHQ-*n* polymers generally showed two transitions on heating and two transitions on cooling. An appreciable hysteresis was always seen between transition temperatures seen on heating and those seen on cooling. It should be noted, however, that the lower temperature transition was seen only on the first heating scan for the polymers with side chains of 6, 8, and 10 carbons. The higher temperature transition was also studied by polarizing optical microscopy, and the transition temperatures seen were in agreement with the DSC results.

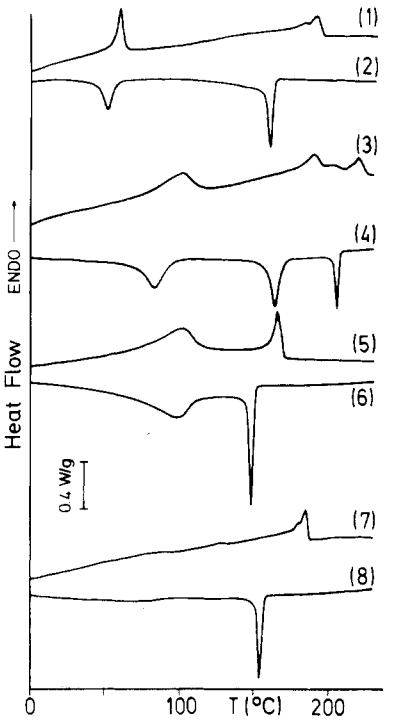

Figure 1. DSC heating and cooling scans taken at 10 °C/min and normalized per gram of sample: curves 1,2, PBCOHQ16; curves 3,4, PTAHQ16; curves 5,6, PTA16HQ16; curves 7,8, PTA16HQ6.

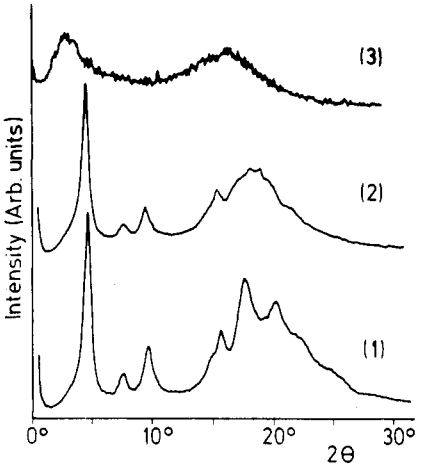

Figure 2. X-ray diffractograms of PBCOHQ16: curve 1, 30 °C; curve 2, 120 °C; curve 3, 220 °C.

X-ray diffractograms were taken of the PBCOHQ-*n* polymers at temperatures corresponding to the different phase regions seen by DSC. Figure 2 shows diffractograms

Table III
Characterization of Polymers from Terephthalic Acid and 2,5-Dialkoxyhydroquinones (PTAHQ-*n*)

				thermal transitions[e]					
		layer spacing		heating			cooling		
n[a]	$[\eta]$[b]	d, Å[c]	d, Å[d]	T_s	T_m	T_i	T_s	T_m	T_i
6	1.20	10.3	11.7	79[f]	275	292		234	279
8	1.71	12.8	14.0	75[f]	255	282		217	256
10	1.21	13.3		78[f]	270			245	
12	0.73	15.5	18.2	78	236		32	181	215
14	0.72[g]	17.6	20.5	91	215	230	62	160	207
16	0.70[g]	19.1	21.8	104	190	215	83	162	202

[a] Number of carbon atoms in the side chain. [b] In dL/g, measured in CH_2Cl_2/TFA (95/5 (v/v)) at 20 °C. [c] Measured at room temperature. [d] Measured at 10 °C below the isotropization temperature. [e] In °C. Heating and cooling rates: 20 °C/min. [f] Transition observed only in the first heating scan. [g] In dL/g, measured in $CHCl_3$/TFA (95/5 (v/v)) at 25 °C.

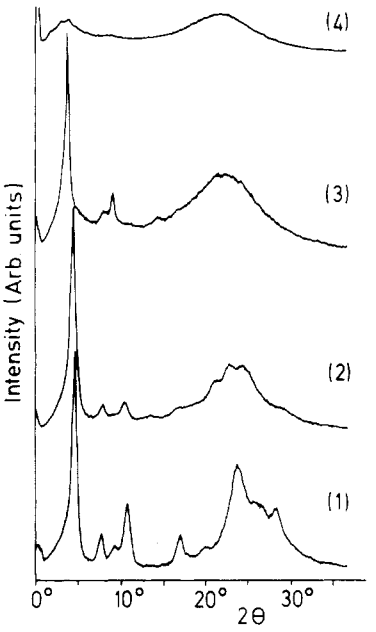

Figure 3. X-ray diffractograms of PTAHQ16: curve 1, 30 °C; curve 2, 140 °C; curve 3, 180 °C; curve 4, 220 °C.

of the PBCOHQ16 polymer at different temperatures. This material is typical of the series, and at 30 °C (curve 1 of Figure 2) the diffractogram consists of three sharp reflections in the small-angle region at spacings of 17.8, 8.8, and 5.8 Å with strong, medium, and weak intensities, respectively. The wide-angle region consists of peaks at spacings of 5.53, 4.93, and 4.33 Å. A peak is also seen at about 11.3 Å. Diffractograms of other homologues of this series generally showed 2 or 3 orders of small-angle reflections with an additional reflection seen at about 11.4 Å and multiple reflections in the wide-angle region. Results of the small-angle spacing for this series at 30 °C after cooling from the melt are summarized in Table II and plotted in Figure 4.

Figure 2, curve 2, shows the diffractogram for the PBCOHQ16 material at 120 °C. Three orders of small-angle reflections are seen with a first order at a spacing of 18.0 Å and the reflection at 11.2 Å. The diffractogram at 220 °C, Figure 2, curve 3, indicates that the material is in the isotropic melt.

PTAHQ-*n* Polymers. A series of PTAHQ-*n* polymers having side-chain lengths of 6, 8, 10, 12, 14, and 16 carbons was also studied. Table III shows the intrinsic viscosities and transition temperatures observed. Figure 1 shows the heating (curve 3) and cooling (curve 4) DSC scans for the PTAHQ16 polymer. This material shows three major transitions on heating and three transitions on cooling. As with the PBCOHQ-*n* materials, about 20 °C of hysteresis was seen between heating and cooling transitions. Polarizing optical microscopy showed that above the second heating transition the material was shearable and birefringent. The last transition on heating corresponded to melting to an isotropic fluid. No textures typical of crystalline or liquid crystalline phases were seen by optical microscopy.

The PTAHQ14 polymer showed also three transitions on heating and three on cooling by DSC. However, the material with 12-carbon side chains was monotropic, showing two transitions on heating and three on cooling, and the PTAHQ10 polymer presented only two transitions on heating and two on cooling. No evidence of a mesophase formation could be seen either by DSC or optical microscopy. Polymers PTAHQ8 and PTAHQ6 showed

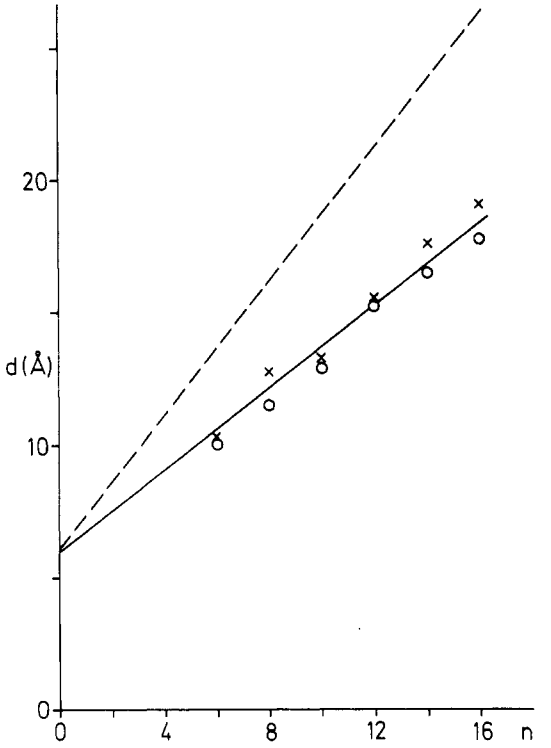

Figure 4. Layer spacings observed by X-ray diffraction as a function of *n*, the number of carbons in the aliphatic side chain: open circles, PBCOHQ-*n* polymers; crosses, PTAHQ-*n* polymers; dashed line, PTA-*n*-HQ melt cooled (from ref 10); solid line, PTA-*n*-HQ solvent precipitated (from ref 10).

again three transitions on heating and three on cooling by DSC.

No evidence of a glass transition was seen in any of these materials.

Figure 3 shows diffractograms of the PTAHQ16 polymer taken at several temperatures. At 30 °C the diffractogram consists of 3 orders of small-angle reflections at spacings of 19.1, 9.4, and 6.2 Å with strong, medium, and weak intensities, respectively. An additional reflection is also seen at a spacing of about 12.7 Å. The wide-angle region consists of reflections at spacings of 5.28, 4.50, and 3.84 Å. Table III summarizes the small-angle spacings seen for other members of the PTAHQ-*n* series at 30 °C after cooling from the melt. These values are plotted in Figure 4. Generally, 2 or 3 orders of small-angle reflections with monotonically decreasing intensities are seen. Additionally, a reflection is generally seen at a spacing of about 12.4 Å, and multiple reflections are seen in the wide-angle region.

Figure 3, curve 2, shows the diffractogram observed for the PTAHQ16 material at 140 °C, below the second cooling transition seen by DSC. The diffractogram again consists of 3 orders of reflections in the small-angle region with a first order at a spacing of 19.6 Å, a reflection at about 12.4 Å, and wide-angle reflections at spacings of 5.01, 4.69, and 4.43 Å. Curve 3 shows the diffractogram taken at 180 °C, below the first DSC cooling transition. Three orders of small-angle reflections are seen, this time with a first order at a spacing of 21.7 Å. An additional reflection is seen at a spacing of about 12.1 Å, and a diffuse halo is seen in the wide-angle region. Curve 4 shows the diffractogram taken at 220 °C indicating the material is in the melt.

Figure 5 shows a plot of diffractograms of PTAHQ16 taken on cooling from the melt at 10 °C temperature intervals to 30 °C. It is clearly seen from the second-order small-angle reflections that the spacing changes discontinuously to lower values at the second cooling transition

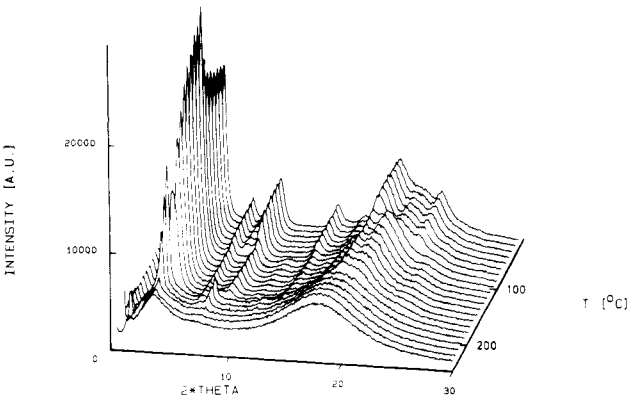

Figure 5. X-ray diffractograms of PTAHQ16 from 230 to 20 °C taken in 10 °C intervals cooling from the melt.

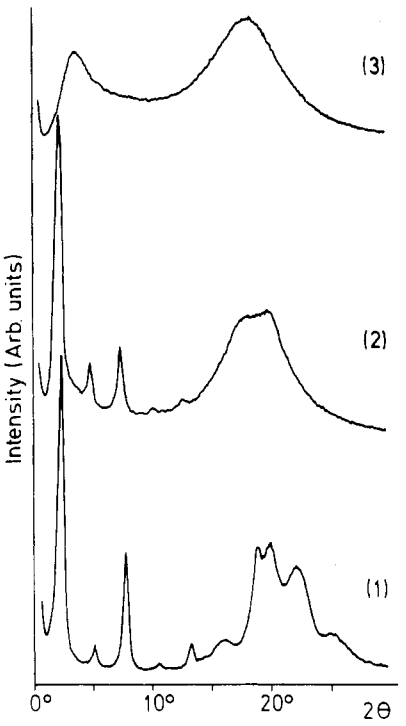

Figure 6. X-ray diffractograms of PTA16HQ16: curve 1, 30 °C; curve 2, 140 °C; curve 3, 200 °C.

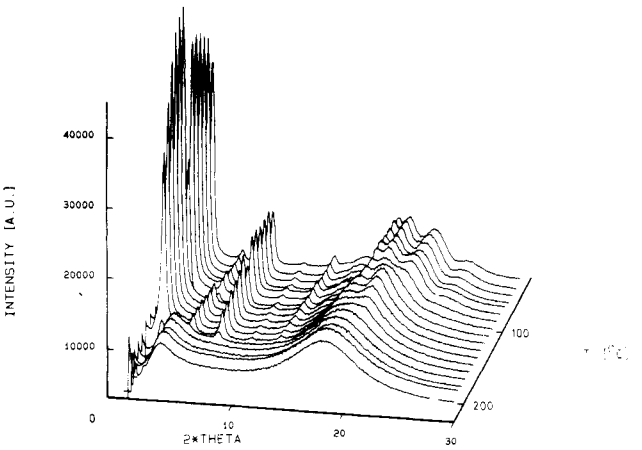

Figure 7. X-ray diffractograms of PTA16HQ16 from 200 to 30 °C taken in 10 °C intervals cooling from the melt.

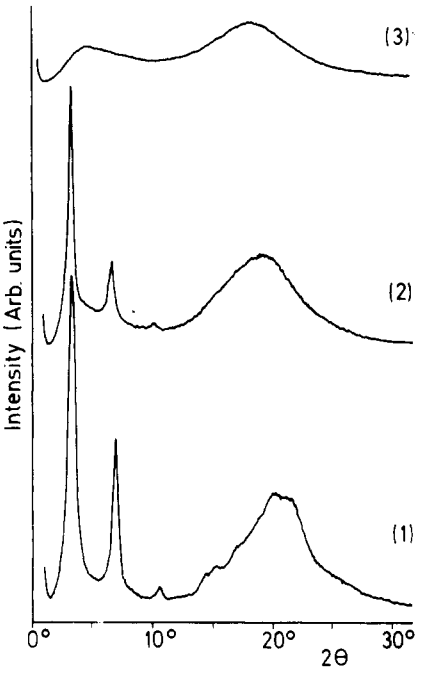

Figure 8. X-ray diffractograms of PTA16HQ6: curve 1, 30 °C; curve 2, 150 °C; curve 3, 230 °C.

and the wide-angle reflections change discontinuously at the third cooling transition. The first-order spacings at temperatures just below isotropization are shown for the entire series in Table III.

PTA16HQ-*n* Polymers. In addition to the PBCOHQ-*n* polymers and PTAHQ-*n* materials, PTA16HQ16 and PTA16HQ6 polymers were prepared. Data are also included from a PTA16HQ polymer prepared elsewhere[25] for reasons of comparison.

The PTA16HQ16 polymer prepared had an intrinsic viscosity of 0.75 dL/g in chloroform/trifluoracetic acid (95/5 (v/v)) at 25 °C. The DSC heating (curve 5) and cooling (curve 6) scans for this polymer are shown in Figure 1. Both curves show two transitions at 102 and 167 °C on heating with about 20 °C of hysteresis seen for the higher temperature transition and the lower temperature transition being rather reversible. Polarization optical microscopy showed that the higher temperature transition corresponded to the formation of an isotropic melt. Also noticed by microscopy was a tendency to form featureless homeotropic textures on cooling from the melt.

X-ray diffractograms taken of the PTA16HQ16 material at various temperatures are shown in Figure 6, curve 1. At 30 °C, 7 orders of small-angle reflections are seen with a first order at a spacing of 32.5 Å and the intensities of the odd reflections being reinforced. The wide-angle region consists of reflections at spacings of 4.4, 4.0, and 3.5 Å. Curve 2 shows the diffractogram taken at 140 °C, below the first cooling transition seen by DSC. The diffractogram consists of 5 orders of reflections with a first order at a spacing of 33.0 Å and a broad reflection in the wide-angle region. Curve 3 Figure 6 shows the diffractogram taken at 200 °C indicating the material is in the isotropic melt. Figure 7 shows a plot of diffractograms taken on cooling this polymer from the melt at 10 °C temperature intervals to 30 °C. This 3-D plot clearly shows the continuous growth of a peak at a spacing of about 4.3 Å on cooling through the high-temperature transition followed by a discontinuous change and the growth of peaks at 4.0 and 3.5 Å on cooling through the low-temperature transition.

The PTA16HQ6 material had an intrinsic viscosity of 1.48 dL/g in chloroform at 25 °C. The DSC scans of this polymer are shown in Figure 1, curves 7 and 8. This material shows two small very broad transitions at about 80 and 125 °C and a large first-order transition at 184 °C on heating and cooling with about 30 °C of hysteresis for

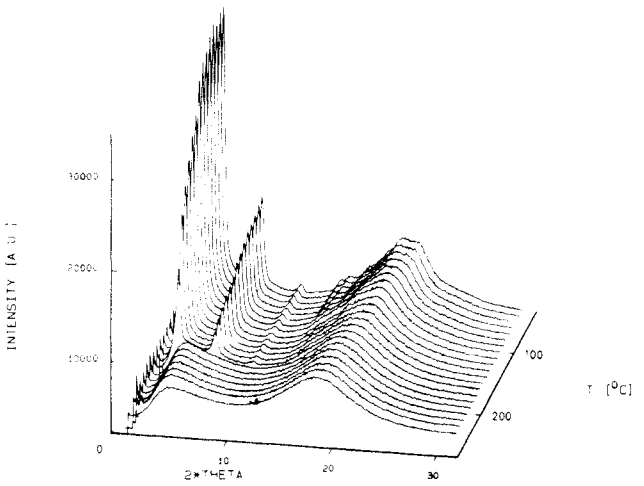

Figure 9. X-ray diffractograms of PTA16HQ6 from 230 to 30 °C taken in 10 °C intervals cooling from the melt.

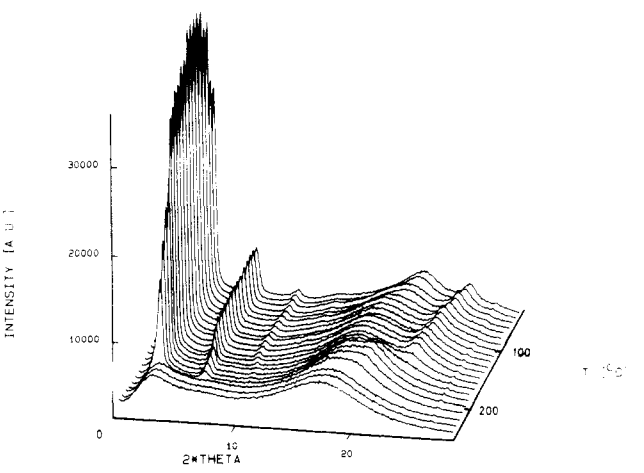

Figure 10. X-ray diffractograms of PTA16HQ from 240 to 30 °C taken in 10 °C intervals cooling from the melt.

the high-temperature transition. Study by polarizing optical microscopy showed that the high-temperature transition seen by DSC corresponded to the formation of the isotropic melt.

X-ray diffractograms taken of the PTA16HQ6 polymer are shown in Figure 8. At 30 °C (curve 1), three orders of small-angle reflections are seen at spacings of 24.6, 12.3, and 8.2 Å with strong, medium, and weak intensities, respectively. In the wide-angle region a rather broad peak reminiscent of a superposition of two peaks is seen. At 150 °C just below the first peak seen by DSC on cooling (curve 2), again 3 orders of small-angle reflections are seen with a first order at 24.6 Å and a broad halo in the wide-angle region. At 230 °C (curve 3), the diffractogram indicates the polymer is in the isotropic melt. Figure 9 shows a series of diffractograms of this polymer at 10 °C intervals on cooling from the melt. From this plot a rather continuous evolution of poorly defined wide-angle peaks on cooling can be seen.

For purposes of comparison, some data for a PTA16HQ polymer are included. This polymer was synthesized in the laboratory of Dr. M. Ballauff, and the batch used for this study is described in ref 25. It had an inherent viscosity of 2.07 dL/g in chloroform at 25 °C measured at a concentration of 0.5 g/dL; synthesis and characterization of this type of PTA-*n*-HQ polymers are described in the literature.[4,5] DSC scans of this polymer after cooling from the melt show three transitions on heating at temperatures of about 45, 140, and 215 °C and three transitions on cooling at about 200, 115, and 35 °C. Reprecipitated material or material crystallized from solution shows a different low-temperature transition occurring at about 100 °C. For material cooled from the melt to 30 °C, X-ray diffractograms from ref 25 show 3 orders of small-angle reflections at spacings of 25.8, 12.7, and 8.5 Å with strong, medium, and weak intensities, respectively. At 30 °C the wide-angle region has several reflections. At 200 °C material cooled from the melt again shows 3 orders of small-angle reflections with a first order at a spacing of 24.1 Å. X-ray diffractograms of PTA16HQ prepared from solvent reprecipitation or crystallization show small-angle reflections with a first order at a spacing of 19.5 Å and multiple wide-angle reflections having different spacings than the melt cooled material. Curves 3 and 4 of Figure 4, taken from ref 10, show the first-order spacing observed from the PTA-*n*-HQ series as a function of side-chain length for melt cooled or reprecipitated material. Figure 10 shows a plot of diffractograms taken at 10 °C intervals on cooling from the melt for this polymer.

Discussion

On the basis of the X-ray results of the PTAHQ-*n* and PBCOHQ-*n* series, several comments can be made.

Firstly, both series show inverse small-angle spacings that go in the ratio 1:2:3 with monotonically decreasing intensities. These spacings increase in a regular way with the number of carbon atoms in the side chain and have quite similar values for corresponding members of both series. This indicates that these materials crystallize in a layered-type structure, as has been seen before for other polyesters having flexible side chains.[10]

Secondly, in the PBCOHQ-*n* series, a reflection is seen at a spacing of about 11.4 Å for all polymers independent of side-chain length; this compares well with the value of about 12 Å measured on space-filling models of the backbone repeat distance. Similarly, a reflection is seen at about 12.7 Å independent of side-chain length for the PTAHQ-*n* series that compares well with the measured repeat value of 12.4 Å.

Thirdly, due to the presence of multiple reflections seen for both series in the wide-angle region at 30 °C, a crystalline structure of the polymers is expected at this temperature.

While a complete description of the structure is difficult only on the basis of information from unoriented samples, it is nonetheless useful to speculate on the structural possibilities for the above polymers.

The simplest possibility would involve a layered structure with the flexible side chains perpendicular to the polymer backbone and interdigitating to give a layer thickness equal to the thickness of the backbone and one fully extended side chain. The problem with such a model is that the layer spacing predicted is much larger than that actually seen by X-ray measurements; the discrepancy is about 6 Å in the case of 16-carbon side chains. Tilting the side chains with respect to the layer plane, one obtains the structure shown schematically in Figure 11a, parts 1 and 2. Taking the extrapolation of the PTAHQ-*n* spacing data shown in Figure 4 to $n = 0$ gives the average bulkiness of the backbone to be about 6 Å. With this backbone thickness and an average carbon–carbon projection distance of about 1.25 Å in the extended ordered state, one can calculate that the tilt angle, Å, for the PTAHQ16 material should be about 41.5°. Considering the measured length of the polymer backbone repeat, this would give a distance between neighboring side chains in the same backbone of about 6.2 Å in the case of PTAHQ-*n* polymers and 5.8 Å in the case of PBCOHQ-*n* polymers. These side-chain lateral approach distances seem unlikely in the

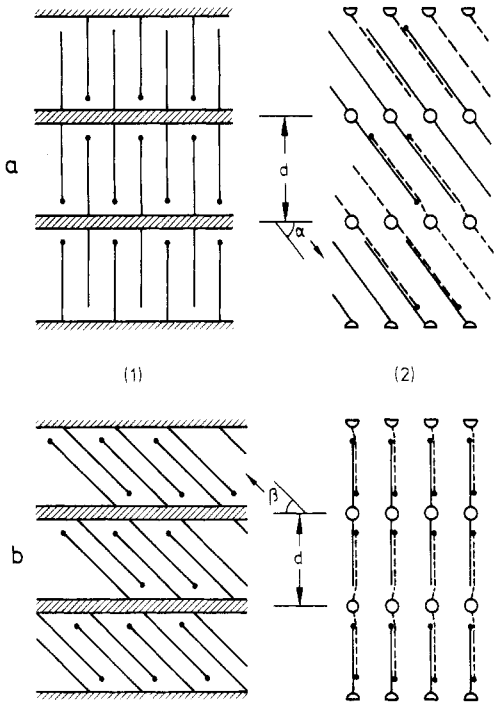

Figure 11. Schematic representation of two possible structural models for PBCOHQ-*n* and PTAHQ-*n* polymers in the solid state showing the packing of the side chains: (a) side chains normal to the backbone; (b) side chains tilted with respect to the backbone.

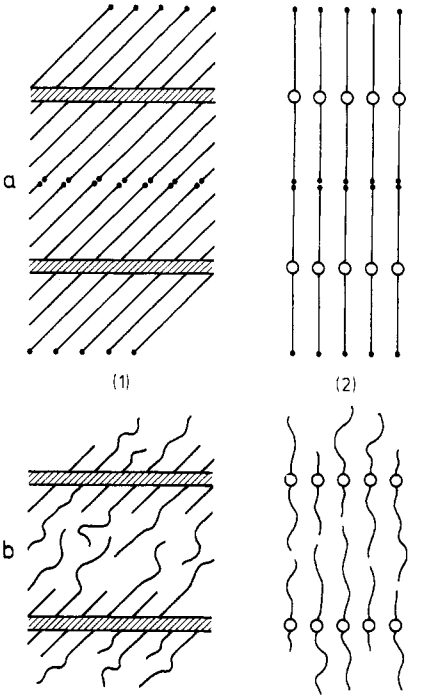

Figure 12. Schematic representation of possible structural models for (a) PTA16HQ16 and (b) PTA16HQ6 polyesters in the solid state showing the packing of side chains.

case of the ordered phases seen here.

A second possibility for layer formation would be to interdigitate side chains and tilt with respect to the axis of the backbone, as shown in Figure 11b, part 1. If the side chains are left perpendicular to the layer plane in the orthogonal direction, one obtains the structure shown in Figure 11b, parts 1 and 2. By use of the same values for backbone thickness and carbon–carbon lengths stated above, a value of the tilt angle, β, of 41.5° can be calculated, and a more reasonable side chain lateral approach distance of about 4.1 Å is found. Of course a herringbone-type arrangement of the side chains would give an identical result, but the geometrical arrangement of the pendent groups from the hydroquinone residue is thought to favor the arrangement shown in Figure 11b. The PBCOHQ-*n* polymers give a very similar result with a slightly smaller lateral approach distance between side chains along the backbone due to the slight difference in the repeat distance.

The real structural situation in both PTAHQ-*n* and PBCOHQ-*n* polymers may involve components of all types of side-chain tilt, but the tilt described above is most likely to dominate.

When polymers of both series are heated above the lower temperature transition seen by DSC, the only changes in the X-ray diffraction patterns take place in the wide-angle region. This can be seen very well on the 3-D plot shown in Figure 5 for the PTAHQ16 polymer. Above the transition, the peaks at 3.84 and 4.5 Å disappear and new peaks at 4.3 and 4.5 Å are seen. Since no changes can be seen in the small-angle region, one must conclude that the layer structure is still maintained, and this transition should correspond to a solid–solid transition, probably due to a disordering process in the side-chain packing. The lower temperature transition has been assigned to the melting of side chains in similar polyesters.[4]

At temperatures above the second DCS transition, the two series of polymers behave differently. In the case of the PBCOHQ-*n* polyester, an isotropic melt is formed, while the PTAHQ-n polymers (except PTAHQ10) melt into a shearable birefringent fluid. The presence of 3 orders of sharp small-angle reflections in the X-ray diffractogram at this temperature and only a broad halo in the wide-angle region indicate the formation of a liquid crystalline mesophase. Here, presumably, the side chains are completely molten while the presence of the reflection at 12.7 Å associated with the backbone repeat suggests that there still exists some correlation between neighboring backbones.

The reasons why PTAHQ10 does not show a mesophase and PTAHQ12 presents a monotropic liquid crystalline transition are still not clear and need further investigation.

Comparing the two series of polyesters, it is seen that while most of the polymers based on terephthalic acid form liquid crystalline mesophases, all polymers from bicyclo-[2,2,2]octane-1,4-dicarboxylic acid do not show a mesophase. Since both the 1,4-bicyclo[2.2.2]octylene and 1,4-phenylene units are considered to be relatively rigid, and at low temperatures, the two series of polymers crystallize in a similar structure. Since both series have similar melting temperatures (especially for longer side chains), there must be reasons other than purely geometrical constraints for mesophase formation. A clear difference in these two units, of course is the presence of polarizable electrons in the 1,4-phenylene moiety, which should lead to intermolecular forces greatly enhancing attraction between the polymeric backbones, thereby stabilizing mesophase formation after melting in the PTAHQ-*n* polymers. Similar conclusions have been reached for low molecular weight materials.[13] This reasoning is also consistent with the observation that the X-ray reflection attributed to the backbone repeat persists in the mesophase.

As seen for the PTAHQ16 polymer in Figure 5 and for other members of the series in Table III, the mesophase formation is accompanied by a rather discontinuous increase in the layer spacing. On the basis of the structural model proposed in Figure 11, one can visualize the mesophase as layers of positionally correlated backbones sep-

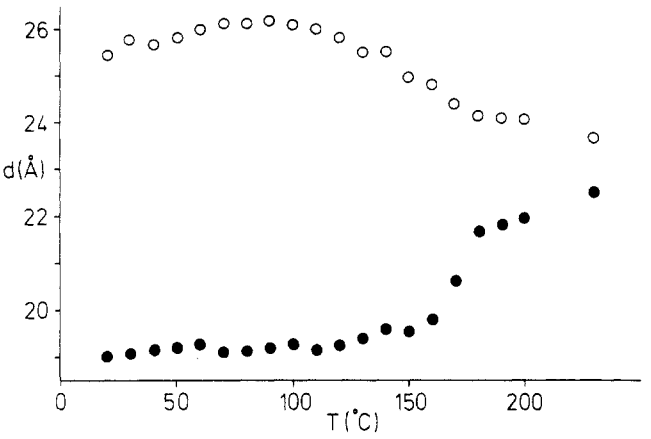

Figure 13. Temperature dependence of the layer spacing of PTAHQ16 (●) and PTA16HQ (○) polymers.

arated by molten side chains. This implies no positional correlation between layers and in this sense is somewhat analogous to low molecular weight smectics A or C. It is fundamentally different than smectics A or C in the sence that the optical director, related to the polarizability of the backbone, should be parallel to the layer plane and the backbones within each layer should be orientationally and positionally correlated.

It is also interesting to compare the behavior of the two polymers PTAHQ16 and PTA16HQ. These two polymers are chemically analogous as they both have the same backbone and the same number of equal length side chains per residue, the only difference being that in the case of the PTAHQ16 polymer the side chains are attached to the hydroquinone residue while in the PTA16HQ they are appended to the terephthalic acid residue.

Both polymers show mesophases on cooling from the melt, yet the structure observed is different between the two. The PTA16HQ polymer on cooling from the mesophase crystallizes into a lamellar structure that has been described[10] as having the side chains extended perpendicular to the backbone and interdigitating with a layer thickness of about 25.8 Å. On the other hand, the PTAHQ16 material crystallizes on cooling from the mesophase into a lamellar structure having the side chains tilted with respect to the backbone (see Figure 11), giving a layer thickness of about 19.1 Å. Furthermore, comparison of the 3-D plots of X-ray diffractograms shown in Figures 5 and 10 for both polymers shows obviously that the PTAHQ16 material is more crystalline at low temperatures.

At higher temperatures both polymers show layered mesophases, but again with different layer spacings, though the difference is smaller than in the crystal. This of course comes from the fact that the layer spacing of the PTA16HQ polymer shows a negative temperature dependence while the PTAHQ16 polymer shows a positive dependence. In fact, as the temperature increases, the spacings tend to converge, as shown in Figure 13. The isotropization temperatures on heating are practically the same for both polymers.

Since the chemical structure of both polymers is so similar, one is driven to ask why the crystalline structures are different. Given the distance between side chains along the backbone, even an interdigitated structure would favor a tilting of the side chains for efficient packing. Therefore, there must be factors hindering the formation of a tilted structure in the case of melt-crystallized PTA16HQ. A possible explanation becomes apparent on looking at molecular models of these two polymers. Considering an alkoxy side chain in an all-trans conformation attached to a terephthalic acid residue in the 2 or 5 position, the least hindered conformation in the plane of the benzene ring is when the side chain is perpendicular to the 1–4 axis. Rotation of the aromatic carbon–oxygen bond by 180°, which would give a tilted side chain with respect to the backbone, is sterically hindered by the hydrogens on the first methylene unit next to the oxygen. In the case of the side chain attached to the hydroquinone unit, this tilt is practically unhindered.

However, a tilted structure has also been observed in the PTA16HQ material when crystallized in the presence of solvent and was also thought to be thermodynamically more stable.[10] Similar tilted phases have also been reported for polyimides containing flexible side chains.[6]

Doubling the number of side chains per repeat unit in the polymer allows a completely different structure to be formed. The powder diffraction pattern for PTA16HQ16 at 30 °C consists of a surprising 7 orders of small-angle reflections. With the reciprocal of the spacings again in the ratio 1:2:3 and multiple wide-angle reflections, this polymer appears to have a well-ordered lamellar structure at this temperature. The observed first-order layer spacing of 32.5 Å is too large for an interdigitated structure like that shown in Figure 11 to be possible. Also, intensity reinforcement of the odd order reflections indicates a pseudoperiodicity of the electron density normal to the layers with a spacing of 16.25 Å. The observed layer spacing is very closely matched, however, by the 32.2 Å obtained from simply doubling the layer spacing value observed for the PTAHQ16 polymer and subtracting the 6-Å value estimated for the backbone by the intercept of Figure 4. A noninterdigitated, tilted structure such as that shown in Figure 12a is expected, as the difference between the PTA16HQ16 polymer and the PTAHQ16 polymer is essentially a doubling of the number of side chains per repeat. This structure explains not only the observed layer spacing but also the oscillation of intensities since a van der Waals gap should be present at the layer surface.

It is interesting to note that the PTA16HQ16 polymer does not show a mesophase, while both PTAHQ16 and PTA16HQ do. The reason for this is expected to lie in the density of side chains per repeat. The presence of four side chains per repeat allows for good geometrical proximity of the side chains for easy crystallization. This, plus the fact that interdigitation of side chains and the accompanying inclusion of chain ends into the crystal is not necessary, allows this polymer to form more ordered layered structures, a fact that is manifested in the 7 orders of X-ray reflections seen in the small-angle region for this polymer compared with only 3 for the others. On the other hand, the volume fraction of side chains is approximately doubled compared to the other materials; thus when they disorder their effect will be much larger, tending to destabilize the mesophase. The extra density of disordered side chains coming from the backbone will tend to push apart adjacent backbones and form an isotropic melt. It should be noted that polymers substituted with one,[7,12] two,[6,10] four, and six[9] flexible side chains per repeat all form different layered mesophases. Presumably in the case of the PTA16HQ16 polymer, the geometry of the substitution is such that crystallization is favored rather than the formation of a mesophase. In the case of six flexible side chains per repeat a mesophase is seen again,[9] with a relatively low clearing temperature but apparently no crysallization. This, however, may well result from the disorder introduced by this very high side-chain density.

A totally different situation is found when the size of the side chains is not the same along the backbone. This is the case for the PTA16HQ6 polymer, in which the size of the side chains alternates between those attached to the terephthalic acid residue, which contains 16 carbon atoms, and those attached to the hydroquinone residue, which has only 6. It can be seen in the DSC traces shown in Figure 1 (curves 7 and 8) for this polymer that the low-temperature transition related to the ordering of the side chains is small and very broad, suggesting a low degree of side-chain order for this polymer. This is expected with side chains of different length. This result is confirmed by the X-ray diffraction patterns shown in Figures 8 and 9, which consists of a broad, poorly defined peak in the wide-angle region at low temperatures. At higher temperatures, an amorphous halo, indicating totally disordered side chains, and 3 orders of reflections in the small-angle region suggest a mesophase with a layered structure, as seen in Figure 12b.

The fact that the layer does not change appreciably on cooling suggests that much of the disorder is just frozen in the solid phase. The difference in side-chain ordering between this material and the PTA16HQ16 polymer is clearly seen in the 3-D plots shown in Figures 7 and 9. Therefore, one can infer from the preceding discussion that in the double-substituted materials having side chains of equal length greatly facilitates crystallization, leading to a stable crystalline phase with long-range ordering that melts directly into an isotropic phase. On the other hand, when the side chains are of sufficiently different lengths, their crystallization is largely suppressed leading to a lower degree of crystallinity and lower melting temperatures but allowing the existance of a wide mesomorphic range. This opens a new and simple way to tailor the mesomorphic properties of these materials.

Experimental Section

Materials and Methods. Bicyclo[2.2.2]octane-1,4-dicarboxylic acid was prepared by the method of Roberts et al.[26] It was purified by several recrystallizations from acetic acid. 2,5-Dihydroxy-*p*-benzoquinone (Aldrich) was dried under vacuum over P_4O_{10}. 1-Alkanols (Fluka) were distilled under vacuum from a 5% solution of their respective sodium alkoxides. Boron trifluoride etherate, acetic anhydride, sodium hyposulfite (all from Fluka), and zinc powder (Merck) were used as received.

All compounds made were characterized by melting point and IR and NMR spectroscopies. Melting points were determined with a Reichert Thermovar melting point microscope and are uncorrected. Infrared spectra were recorded with a Perkin Elmer 1430 IR spectrophotometer. ^1H and ^{13}C NMR spectra were obtained with a Bruker AC 300 spectrometer.

Differential scanning calorimetry (DSC) was performed by using a Mettler DSC-30 and a Perkin Elmer DSC-7 instruments. X-ray diffraction patterns were recorded with a Siemens D500 diffractometer in the reflection mode with Ni-filtered Cu Kα radiation and are uncorrected.

Intrinsic viscosities [η] of the polymers were determined with an Ubbelohde viscometer at 20 °C in methylene chloride/trifluoroacetic acid (95/5 (v/v)) unless otherwise stated.

2,5-Dialkoxy-*p*-benzoquinones. In a three-neck flask equipped with reflux condenser, inert gas inlet, dropping funnel, and magnetic stirring were placed 2,5-dihydroxyquinone (0.07 mol) and the corresponding 1-alkanol (0.4 mol, large excess). The reaction mixture was heated to 40–80 °C (depending on the melting point of the alcohol), and boron trifluoride etherate (0.14 mol) was added dropwise. The mixture was kept stirring at this temperature under Ar atmosphere for 20 h. After the reaction time, it was diluted with approximately 200 mL of methanol and cooled to 0 °C, and the crystallized product was filtered off, washed with acetone, and dried under vacuum at room temperature. Bright-yellow crystals of 2,5-dialkoxybenzoquinones were obtained.

2,5-Dialkoxyhydroquinones. The 2,5-dialkoxybenzoquinone was dissolved in a minimum amount of boiling ethanol, and a 10-fold excess of $Na_2S_2O_4$ (10% aqueous solution) was added dropwise with vigorous stirring. A white product precipitated immediately. The mixture was stirred for 5 min more, and then the product was filtered, washed with water several times, and dried. It was then recrystallized from toluene, washed with cyclohexane, and dried under vacuum over P_4O_{10} at room temperature. White crystals of 2,5-dialkoxyhydroquinones were obtained.

2,5-Dialkoxyhydroquinone Diacetates. The 2,5-dialkoxybenzoquinone was dissolved in acetic anhydride by warming the mixture to 70 °C under Ar atmosphere. Zinc dust was added in small portions with vigorous stirring until the yellow color of the solution disappeared (usually 2–4 h). The reaction mixture was then filtered hot to remove the Zn and poured into ice water with stirring to hydrolyze the anhydride. The white product precipitated was filtered off and dried under vacuum at room temperature. It was further purified by recrystallization from cyclohexane. The 2,5-dialkoxyhydroquinone diacetates were obtained as white crystalline compounds.

Polymers of Bicyclo[2.2.2]octane-1,4-dicarboxylic Acid. Stoichiometric amounts of bicyclo[2.2.2]octane-1,4-dicarboxylic acid and 2,5-dialkoxyhydroquinone diacetate were placed into a polymerization tube equipped with magnetic stirring, inert gas inlet/outlet, and vacuum inlet. The tube was evacuated and then filled with Ar. This cycle was repeated 4 times, and then a slow stream of Ar was maintained in the tube to carry off the acetic acid produced during the polymerization. The tube was immersed in an oil bath at 250 °C, and the melt was stirred at this temperature until all the diacid was dissolved in the molten hydroquinone monomer (usually 1 h). Then the temperature was raised slowly to 280 °C and the melt kept at this temperature until it was so viscous that it could no longer be stirred (usually 1–2 h). Finally, vacuum (2×10^{-2} mbar) was applied to the tube at this temperature for one more hour. After cooling to room temperature, the polymer was dissolved in a chloroform/trifluoracetic acid mixture (95/5 (v/v)) and precipitated into methanol. The polymer was then filtered, extracted in a Soxhlet for 24 h with methanol, and dried under vacuum at room temperature.

Polymers of Terephthalic Acid. After stoichiometric amounts of terephthaloyl chloride and 2,5-dialkoxyhydroquinone were placed into a polymerization tube and treated as described before for the bicyclo[2.2.2]octane polymers, the tube was heated in an oil bath to 160 °C and a low stream of Ar was passed over the melt to sweep out the HCl evolved. As the melt became more viscous, the temperature was raised slowly to 280 °C (approximately 2 h). Then when the melt could not be stirred anymore, vacuum was applied, and the melt was kept at this temperature for 1 h. The polymers obtained were isolated and purified as described above for the bicyclo[2.2.2]octane polyesters.

Acknowledgment. We are indebted to Drs. M. Ballauff and Ch. Kröhnke for helpful discussions and suggestions throughout the course of this work. The technical assistance of F.-P. Gramlich and A. Reichert in the preparative part of this work is greatly appreciated. Financial support, in terms of scholarships, from the Max-Planck-Gesellschaft and in part by E. I. du Pont de Nemours & Co. is gratefully acknowledged.

Registry No. **1** (n = 6), 118476-22-5; **1** (n = 8), 118476-23-6; **1** (n = 10), 51767-60-3; **1** (n = 12), 118476-24-7; **1** (n = 14), 118476-25-8; **1** (n = 16), 118476-26-9; **2** (n = 6), 118476-31-6; **2** (n = 8), 118476-32-7; **2** (n = 10), 118476-33-8; **2** (n = 12), 118476-34-9; **2** (n = 14), 118476-35-0; **2** (n = 16), 118476-36-1; **3** (n = 6), 41505-36-6; **3** (n = 8), 118476-27-0; **3** (n = 10), 118476-28-1; **3** (n = 12), 118476-29-2; **3** (n = 14), 118476-30-5; **3** (n = 16), 115563-53-6; PBCOHQ-6 (copolymer), 118476-49-6; PBCOHQ-6 (SRU), 118476-37-2; PBCOHQ-8 (copolymer), 118476-50-9; PBCOHQ-8 (SRU), 118476-38-3; PBCOHQ-10 (copolymer), 118476-51-0; PBCOHQ-10 (SRU), 118476-39-4; PBCOHQ-12 (copolymer), 118476-52-1; PBCOHQ-12 (SRU), 118476-40-7; PBCOHQ-14 (copolymer), 118476-53-2; PBCOHQ-14 (SRU), 118476-41-8; PBCOHQ-16 (copolymer), 118476-54-3; PBCOHQ-16 (SRU), 118476-42-9; PTAHQ-6 (copolymer), 118476-55-4; PTAHQ-6 (SRU), 118476-43-0; PTAHQ-8 (copolymer), 118476-

56-5; PTAHQ-8 (SRU), 118476-44-1; PTAHQ-10 (copolymer), 118494-16-9; PTAHQ-10 (SRU), 118476-45-2; PTAHQ-12 (copolymer), 118476-57-6; PTAHQ-12 (SRU), 118476-46-3; PTAHQ-14 (copolymer), 118476-58-7; PTAHQ-14 (SRU), 118476-47-4; PTAHQ-16 (copolymer), 115563-54-7; PTAHQ-16 (SRU), 115563-57-0.

References and Notes

(1) Jackson, W. J. *Br. Polym. J.* **1980**, *12*, 154.
(2) Krigbaum, W. R.; Hakemi, H.; Kotek, R. *Macromolecules* **1985**, *18*, 965.
(3) Majnusz, J.; Catala, J. M.; Lenz, R. W. *Eur. Polym. J.* **1983**, *19*, 1043.
(4) Ballauff, M. *Makromol. Chem., Rapid Commun.* **1986**, *7*, 407.
(5) Ballauff, M.; Schmidt, G. F. *Makromol. Chem., Rapid Commun.* **1987**, *8*, 93.
(6) Wenzel, M.; Ballauff, M.; Wegner, G. *Makromol. Chem.* **1987**, *188*, 2865.
(7) Berger, K.; Ballauff, M. *Mol. Cryst. Liq. Cryst.* **1988**, *157*, 109.
(8) Ringsdorf, H.; Tschirner, P.; Herrmann-Schönherr, O.; Wendorff, J. H. *Makromol. Chem.* **1987**, *188*, 1431.
(9) Herrmann-Schönherr, O.; Wendorff, J. H.; Ringsdorf, H.; Tschirner, P. *Makromol. Chem., Rapid Commun.* **1986**, *7*, 791.
(10) Ballauff, M.; Schmidt, G. F. *Mol. Cryst. Liq. Cryst.* **1987**, *147*, 163.
(11) Ballauff, M. *Macromolecules* **1986**, *19*, 1366.
(12) Braun, D.; Hirschmann, H.; Hermann-Schönherr, O.; Lienert, M.; Wendorff, J. H. *Makromol. Chem., Rapid Commun.* **1988**, *9*, 309.
(13) Dewar, M. J. S.; Goldberg, R. S. *J. Am. Chem. Soc.* **1970**, *92*, 1582.
(14) Dewar, M. J. S.; Riddle, R. M. *J. Am. Chem. Soc.* **1975**, *97*, 6658.
(15) Dewar, M. J. S.; Griffin, A. C. *J. Am. Chem. Soc.* **1975**, *97*, 6662.
(16) Carr, N.; Gray, G. W.; Kelly, S. M. *Mol. Cryst. Liq. Cryst.* **1981**, *66*, 267.
(17) Gray, G. W.; Kelly, S. M. *Mol. Cryst. Liq. Cryst.* **1981**, *75*, 95.
(18) Taimr, L.; Smith, J. G. *J. Polym. Sci. Polym. Chem. Ed.* **1971**, *9*, 1203.
(19) Polk, M. B.; Onwumere, F. C. *J. Macromol. Sci., Chem.* **1986**, *A23*, 423.
(20) Polk, M. B.; Nandu, M.; Phingbodhipakkiya, M. *J. Polym. Sci., Polym. Chem. Ed.* **1986**, *24*, 1923.
(21) Polk, M. B.; et al. *Mol. Cryst. Liq. Cryst.* **1988**, *157*, 1.
(22) Crosby, A. H.; Lutz, R. E. *J. Am. Chem. Soc.* **1956**, *78*, 1233.
(23) Baker, W. J. *J. Chem. Soc.* **1941**, 662.
(24) Wegner, G. In *Polymere Werkstoffe*; Batzer, H. Ed.; Verlag Thieme: Stuttgart, 1985; Vol. 1.
(25) Duran, R.; Ballauff, M.; Wenzel, M.; Wegner, G. *Macromolecules* **1988**, *21*, 2897.
(26) Roberts, J. D.; Moreland, W. T.; Frazer, W. *J. Am. Chem. Soc.* **1953**, *75*, 637.

Systems Containing Two Oppositely Charged Polyelectrolytes. Behavior of Ionic Photosensitizers and Quenchers

Gad S. Nahor and Joseph Rabani*

Energy Research Center and The Department of Physical Chemistry, The Hebrew University of Jerusalem, Jerusalem 91904, Israel.

Received June 30, 1988; Revised Manuscript Received November 7, 1988

ABSTRACT: Several photosensitizer–quencher systems containing both the negative polyelectrolyte poly(styrenesulfonate) (PSS) and the positive polyion polybrene (PB) have been investigated. At relatively low concentrations, solutions containing both PSS and PB are stable with respect to precipitation even at equivalent concentrations. Interactions of the polyelectrolytes with the photosensitizer zinc tetrakis(sulfonatophenyl)porphyrin ($ZnTPPS^{4-}$) and *meso*-tetrakis(*N*-methylpyridinium-4-yl)porphyrin, $ZnTMPyP^{4+}$, have been studied by spectrophotometric and spectrofluorimetric techniques. The concentration effect of the PSS induces the formation of charge-transfer complexes between a photosensitizer and the hydrophobic parts of the polymer, as well as photosensitizer dimers. The effects of the oppositely charged polyion on the absorption and emission spectra of the photosensitizers as well as the effect of several quenchers have been studied. The results lead to the conclusion that each of the two polyelectrolytes preserves part of its electrical field in its vicinity even when the oppositely charged polymer is in slight excess.

Introduction

Although mixing two solutions containing oppositely charged polyelectrolytes usually results with precipitation, there are well-known cases where the polymeric components remain in solution. Studies concerning the preparation, stability, and kinetic properties of polyelectrolyte complexation have been reported.[1-16] The term "complexation" in this context refers to the formation of pairs of the two oppositely charged polymers. Application of such complexes to other fields, such as medicine[17-19] and membrane science,[20-23] has been reported.

In the present manuscript we report the behavior of ionic photosensitizers and quenchers in a polyelectrolyte complex composed of poly(styrenesulfonate) (PSS) and polybrene (PB). This research has a potential importance in the application of microenvironments for the purpose of photochemical conversion and storage of light energy.

Experimental Section

Absorption spectra have been recorded by using a Bausch and Lomb Spectronic 2000 spectrophotometer. Emission was measured with a Perkin-Elmer LS-5 spectrofluorimeter. Laser photolysis was carried out with a Molectron DL200 dye laser, 450 μJ, 10-ns fwhm, pumped by a Molectron UV N_2 laser. The irradiation cell was 1 cm long. The analytical light and laser beam were oppositely coaxial as previously described.[24-26] The resolution time of this setup under our conditions was 2 μs. A 150-W Xe lamp was used as the analytical light source. The signal was transferred through a B&L monochromator to an IP28 photomultiplier and was digitized with a Tektronix 7912 AD digitizer.

Materials. All reagents were of the highest purity available. The sodium salt of $TPPS^{4-}$ and $TMPyP^{4+}$ (chloride form) were products of Strem Chemical Inc. and used as received. The Zn complex $ZnTPPS^{4-}$ was prepared and purified according to the method of Cheung et al.[27] $ZnTMPyP^{4+}$ was prepared according to the previously described procedure.[28] PB, as a bromide, was purchased from Sigma and was used as received. Poly(styrenesulfonate) (PSS), completely sulfonated, MW 70 000, in the sodium salt form was purchased from Polysciences. It was purified by dialysis against 10^{-3} M EDTA followed by dialysis against water. Water was purified by passing through an ion exchanger, distilled, and finally passed through a Millipore Milli-Q water purification system. The temperature was 23 ± 2 °C. Polymer concentrations are given in terms of the monomer units.

Results and Discussion

When charge-equivalent concentrations of PSS and PB solutions are mixed together, turbidity is instantly pro-

0024-9297/89/2222-2516$01.50/0